Chemistry & Biology, Vol. 10, 123–130, February, 2003, ©2003 Elsevier Science Ltd. All rights reserved. DOI 10.1016/S1074-5521(03)00019-X

Selective Chemical Treatment of Cellular Microdomains Using Multiple Laminar Streams

Shuichi Takayama,[1] Emanuele Ostuni,[1] Philip LeDuc,[2] Keiji Naruse,[2] Donald E. Ingber,[2,*] and George M. Whitesides[1,*]
[1]Department of Chemistry and Chemical Biology
Harvard University
12 Oxford Street
Cambridge, Massachusetts 02138
[2]Department of Pathology and
Department of Surgery
Children's Hospital and
Harvard Medical School
Boston, Massachusetts 02115

Summary

There are many experiments in which it would be useful to treat a part of the surface or interior of a cell with a biochemical reagent. It is difficult, however, to achieve subcellular specificity, because small molecules diffuse distances equal to the extent of the cell in seconds. This paper demonstrates experimentally, and analyzes theoretically, the use of multiple laminar fluid streams in microfluidic channels to deliver reagents to, and remove them from, cells with subcellular spatial selectivity. The technique made it possible to label different subpopulations of mitochondria fluorescently, to disrupt selected regions of the cytoskeleton chemically, to dislodge limited areas of cell-substrate adhesions enzymatically, and to observe microcompartmental endocytosis within individual cells. This technique does not require microinjection or immobilization of reagents onto nondiffusive objects; it opens a new window into cell biology.

Introduction

Complex phenotypic behaviors of cells—mitosis, growth, motility, metabolism, differentiation, and apoptosis—reflect the integration of processes occurring in spatially distinct microdomains [1, 2]. Analysis of cellular control, therefore, requires methods that can perturb or manipulate structural domains within single living cells, with high molecular selectivity and with micron-scale spatial accuracy. A number of mechanical or optical techniques are currently used for micromanipulation of cells, but these techniques all have limitations. For example, micromanipulation using optical tweezers [3] can provide subcellular spatial resolution but has limited molecular specificity. Target-specific small-molecule reagents can provide molecular specificity but lack spatial control at the subcellular level. The rapid diffusion of small molecules inside cells (typical intracellular diffusion coefficient $D = 1 \times 10^{-6}$ cm^2/s) and the small size of surface attached cells (typically 5–100 μm) makes localization of reagents intrinsically difficult. Light-triggered activation of photosensitive reagents that generate bioactive molecules upon photolysis (caged molecules) can be performed with subcellular resolution [4], but the localization is short lived, again due to rapid diffusion [5]. Reagents can be immobilized onto nondiffusive objects such as microspheres to localize delivery [6]; immobilization may, however, perturb cellular physiology. Currently, there are two techniques that can localize rapidly diffusing small molecules to subcellular domains: Bradke and colleagues have developed a method in which they used two pipettes—one to dispense liquid and one to remove liquid—to treat part of a neurite outgrowth locally with a small-molecule drug [7]. This method accomplishes the goal of localizing small molecules to subcellular regions; however, Bradke's method requires precise handling of micromanipulators, and the fluid flow may be susceptible to disturbances and variations because the experiments are performed in a nonenclosed, open fluidic system. We have developed a different technique (for brevity, we call the technique "PARTCELL," *par*tial *t*reatment of *cell*s using laminar flows) that can deliver small-molecule reagents to cells and remove these reagents from cells with subcellular resolution inside closed channel systems, without the requirement of micromanipulation; using PARTCELL, we demonstrated localization of two different chemicals to two different subcellular domains [8]. In this paper, we define a theoretical framework for the intracellular chemical localization process of PARTCELL to investigate its experimental scope and limitations, and we further extend the experimental demonstrations to selective treatment of specific areas of cell surfaces.

PARTCELL uses parallel laminar streams of different liquids flowing inside a capillary network; these streams are generated by combining flows from multiple inlets. In small (hundreds of microns) channels with slow flow ($v \approx 0.6$ cm/s, as calculated by volume displacement per time), the Reynolds number (Re) is small (<1), and the streams of fluids flow next to each other without mixing, other than by diffusion; that is, there is no turbulence (Figure 1). Multiple laminar flow systems have previously been utilized to perform separations [9–11], in sensors [12], to fabricate microstructures in capillaries [13, 14], and to pattern cells and their environments [8, 13, 15, 16]. In PARTCELL, the interface between adjacent liquid streams is positioned over a single living cell to expose different regions of the cell to different streams; this localized exposure allows treatment of subcellular domains of the cell [8]. We illustrate the application of PARTCELL to the study of phenomena occurring at the subcellular level with studies of four processes: (1) labeling of mitochondria with fluorophores; (2) disruption of cytoskeletal filaments using a membrane-permeable, small molecule that binds to actin monomers; (3) detachment of a cell from its substrate using trypsin; and (4) receptor-mediated endocytosis.

Results and Discussion

Figure 1 outlines a representative experiment. We fabricated a capillary system having three inlet channels that

*Correspondence: gwhitesides@gmwgroup.harvard.edu (G.M.W.), donald.ingber@tch.harvard.edu (D.E.I.)

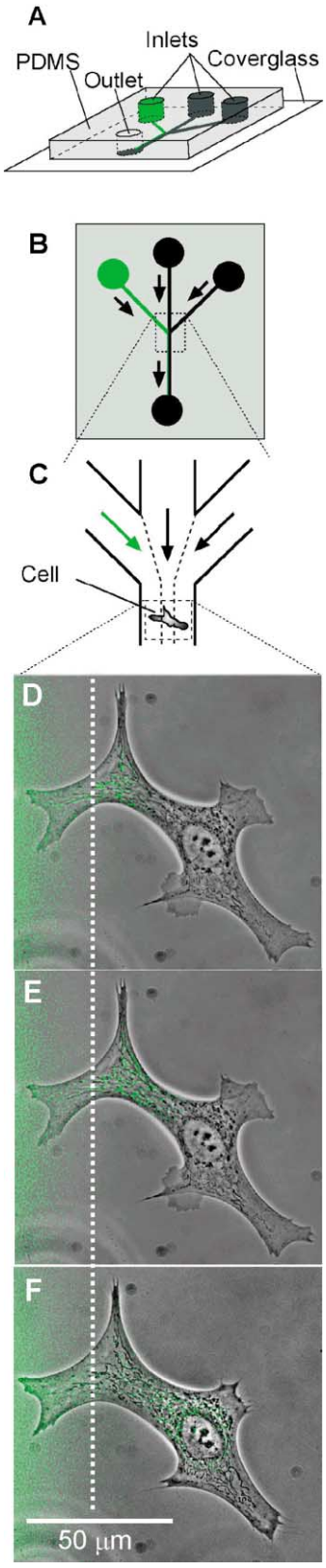

Figure 1. Use of PARTCELL to Generate Two Spatially Localized Populations (Fluorescently Labeled and Unlabeled) of Mitochondria Using Mitotracker Green within a Single BCE Cell

converge into a single main channel by placing a poly (dimethylsiloxane) (PDMS) slab with channel features molded into its surface on a glass cover slip (Figure 1A) [16]. Parallel streams of different liquids are created in the main channel by allowing individual solutions to flow from the inlets (Figures 1B and 1C). Although the exact width and shape of the interface will depend on flow velocity, channel geometry, wall interactions, and the diffusion coefficient of the reagent of interest [17–19], in the experiments described here the interface between the liquid streams is typically 1–10 μm in width in the region where cells are treated (50–300 μm from the point where the different flows converge). The entrance length is ~100 μm in our system. Thus, most of our experiments were performed in the regime where fluid flow is fully developed. The width of each stream, and the position of the interface between adjacent streams, is controlled by adjusting the relative amounts of fluid flowing in from each inlet. We position the interface between two adjacent streams—one containing and one lacking a molecule of interest—over a mammalian cell anchored to the floor of the channel (Figure 1C). We have previously reported the use of this process to selectively label two different subpopulations of mitochondria in opposite ends of a living bovine capillary endothelial (BCE) cell using a 3 min exposure of the cell to Mitotracker Green and Red [8]. To study the experimental scope of the mitochondria labeling procedure in more detail, we subjected a cell to a Mitotracker Green FM solution over a more extended period of time. Figures 1D–1F show the different extent of labeling after 5, 11, and 35 min of PARTCELL treatment with Mitotracker Green FM, a molecule that labels mitochondria irreversibly. The extent of intracellular staining progressed most rapidly (~10 μm/min) in the first minute of exposure to Mitotracker solution and then slowed down considerably. After repeated excitation, we observed selective photobleaching in mitochondria that were labeled first and had the highest intensity of labeling (Figure 1F). These observa-

(A) Schematic representation of a typical setup for a PARTCELL experiment. A poly(dimethylsiloxane) (PDMS) membrane containing micron-sized channels molded in its surface was placed on the flat surface of a cover glass to form a network of capillaries. Fluids were pumped by gentle aspiration at the outlet, or by adding different levels of fluids in the inlet and outlet reservoirs to create pressure differences using gravitational forces.
(B) A top view of the channel system.
(C) A close-up view of the area where the inlet channels combine into one main channel. Different streams of fluids were allowed to flow over different regions of a single cell.
(D) An overlay of fluorescence (green: 488 nm excitation, FITC filter, dehazed and color enhanced to reproduce original colors) and phase-contrast images taken after a Mitotracker Green FM solution (3 μM in medium) was allowed to flow over the left portion of the cell and medium was allowed to flow over the right portion of the cell for 5 min. The white dotted line indicates the position of the interface between the flows with and without Mitotracker Green. Mitotracker diffused to different extents into the cell beyond the boundary defined by the fluid streams with time.
(E) A fluorescence image taken after 11 min of continuous flow of Mitotracker Green FM solution over the left half of the cell. The phase image from (D) (different time point) was overlayed for reference.
(F) An overlay image taken after 35 min of continuous flow of Mitotracker Green FM solution over the left half of the cell.

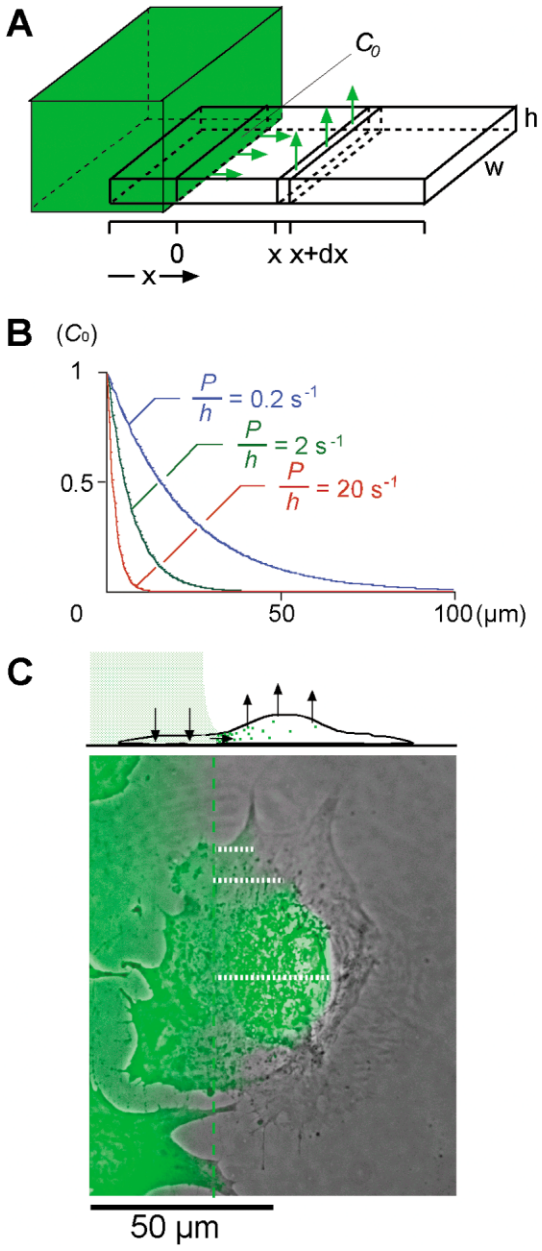

Figure 2. Theoretical Analysis of Intracellular Concentration Gradients Generated by PARTCELL

(A) A semi-infinite rectangular cell of width w and height h, infinitely long in the x direction, was used as a model for theoretical analysis (see Equation 2). The left portion of the cell was exposed to a flow containing the molecule of interest, and the right portion was exposed to a flow that did not contain the molecule. Concentration gradients were considered only in the x direction; concentration gradients across the height of the cell were not considered, because cells spread onto a channel floor have small heights, and diffusive mixing across this distance is expected to be fast (in other words, our model applies for systems with $PhD^{-1} << 1$). Because the cell is thin and spread out ($hw^{-1} << 1$), we also made an approximation that the efflux of molecules occurs only through the apical membrane of the cell. The intracellular concentration of the molecule of interest at $x = 0$ (the initial point in the x direction where the concentration of the molecule of interest outside the cell becomes negligible) is designated C_0.

(B) Steady-state intracellular concentration gradients generated by PARTCELL at various ratios of permeabilities (P) (cm/s) to cell heights (h) (cm) of a molecule with $D = 1 \times 10^{-6}$ cm^2/s, calculated using Equation 3.

(C) Overlay of fluorescence (color enhanced to reproduce original color) and phase-contrast images of a BCE cell at steady-state staining (18 min) with Syto 9 (60 μM). The actual shape of the cell and the interface between the different streams is more complex than the simplified model in (A). However, as expected from the theoretical analysis, which relates intracellular concentration gradients with cell thickness, intracellular diffusion is greater around the nucleus, where the cell is thicker, than in the periphery, where the cell is thinner. The green dotted line represents the interface between the flows with and without Syto 9. The white dotted lines represent the extent of intracellular diffusion at different regions of the cell, as determined by the minimum fluorescence signal detected in our imaging system.

tions show the ability of PARTCELL to localize chemicals to subcellular domains for extended periods of time and also suggests the possible use of PARTCELL for novel subcellular photodynamic experiments where light exposure is global but the labeling is localized (traditional photodynamic experiments use global labeling and localized light exposure instead [20, 21]).

A small molecule having a typical intracellular diffusion coefficient (MW $\sim$ 600, $D \sim 1 \times 10^{-6}$ cm^2/s in cytoplasm) will diffuse $\sim$110 μm (that is, more than the total length of a typical cell) in 1 min [22]. Microinjection and fluorescence recovery after photobleaching (FRAP) studies have shown that small molecules diffuse throughout the cytoplasm within seconds [5, 23] and reach 95% of the final distribution within 2–5 min in 130 μm long mammalian cells, even in the presence of some reversible association of the molecule to immobile cellular components. We also performed microinjection-diffusion experiments using Sulforhodamine 101 acid chloride (Texas Red, Sigma; 5 μM in CO_2-independent media) and observed rapid (tens of seconds) intracellular diffusion in BCE cells (data not shown). PARTCELL can, however, maintain significant intracellular concentration differences of membrane-permeable small molecules inside adherent mammalian cells for prolonged periods.

To determine the scope of the intracellular chemical localization procedure of PARTCELL in more detail, we derived a mathematical description of the intracellular concentration gradient generated by PARTCELL in a simplified model cell (Figure 2A), for molecules that do not interact or that interact reversibly to immobile cellular components. The common form of the one-dimensional diffusion equation [24] that includes the additional membrane-limited efflux of molecules from the boundary at the rate r is given by Equation 1. In PARTCELL, we assume $r = Pc$; substitution into Equation 1 gives Equation 2. In Equation 2, D (cm^2/s) is the diffusion coefficient, c (molecules/cm^3) is the concentration of the molecule, P (cm/s) is the membrane permeability of the molecule as it diffuses out of the cell, and h (cm) is the height of the cell (assumed to be a rectangular slab). With boundary conditions of $c_0 = C_0$ and $c_\infty = 0$—that is, c at $x = 0$ is always C_0, and c at $x = \infty$ is always 0—one obtains an analytical solution for the concentration gradient at steady state ($\partial c/\partial t = 0$) given by Equation 3 [24].

$$\left(\frac{\partial c}{\partial t}\right) = \text{rate of accumulation/volume} = D\frac{\partial^2 c}{\partial x^2} - \frac{r}{h} \quad (1)$$

$$\frac{\partial c}{\partial t} = D\frac{\partial^2 c}{\partial x^2} - \frac{P}{h}c \quad (2)$$

$$c = C_0 e^{-x(Ph^{-1}D^{-1})^{1/2}} \quad (3)$$

This analysis does not rely on (or take into account) any reduction in apparent diffusion rates that may occur by binding of molecules to immobile components within a cell, or due to geometric barriers [5, 24, 25]. The equation for the steady-state concentration gradient (Equation 3), however, is also valid for reversibly interacting molecules, because, if the concentration of molecules bound to immobile cellular components is S [24], then

$$\frac{\partial c}{\partial t} = D\frac{\partial^2 c}{\partial x^2} - \frac{P}{h}c - \frac{\partial S}{\partial t} \quad (4)$$

and the steady-state solution ($\partial c/\partial t = 0$, $\partial S/\partial t = 0$) is still Equation 3.

Figure 2B shows results calculated for several values of Ph^{-1} for steady-state intracellular concentration gradients generated by PARTCELL within a model cell using a typical, rapidly diffusing, small molecule that has no interaction or reversible interactions with immobile cellular components. These calculated results predict that PARTCELL should be broadly applicable to small-molecule/membrane combinations with a wide range of permeabilities (P) (from 1 to 10^{-5} cm/s) in substrate-attached cells (adherent mammalian cells generally have a maximum cell height of $\sim$5 μm when well spread on a rigid substrate), albeit with different degrees of chemical localization. Equation 3 also predicts that the spatial confinement of high concentrations of small molecules in a cell increases with increasing permeability, decreasing thickness of the cell, and decreasing diffusion coefficient of the molecule within the cell (Figure 2B).

Figure 2C illustrates, experimentally, the relationship between the intracellular diffusion of molecules and cell thickness at steady-state staining; here, a BCE cell was stained with Syto 9, an RNA/DNA intercalating stain. Syto 9 has two important properties useful for experimentally testing the theoretical model: it binds reversibly to intracellular components, and it increases fluorescence upon binding. It is necessary to use a dye that is faint in solution but becomes bright once "inside" the cell to observe the intracellular diffusion of dye molecules at the same time there is actual flow of concentrated reagent solution over the cell. Otherwise, the bright fluorescence from the reagent delivery stream, which has many more molecules, drowns out any weak signals from the few molecules inside the cell. At steady-state staining with Syto 9, the stained region of the cell extends only a small distance from the stream of staining solution at the cell periphery where it is thin, but extends further to the right in the thicker parts of the cell around the nucleus (Figure 2C, white dotted lines). This staining pattern reflects differences in the ratio of molecules leaving the cell to molecules diffusing within the cell in these regions; this ratio is high in the thin parts of cells and lower in the thick regions, as predicted by theoretical analysis.

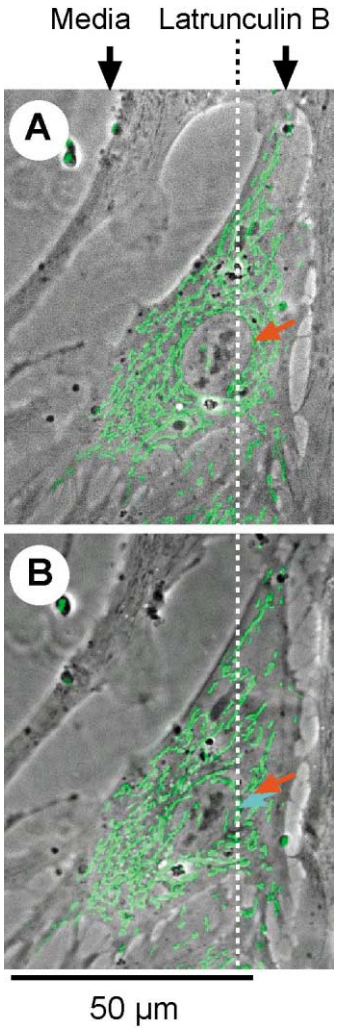

Figure 3. Disruption of Actin Filaments and Displacement of Mitochondria Induced by Treatment of a Portion of a Single BCE Cell with Latrunculin B, a Filamentous Actin-Disrupting Drug

(A) An overlay of phase-contrast and fluorescence (color enhanced to reproduce original colors) images of a BCE cell and its mitochondria prior to the addition of latrunculin B. The white dotted line indicates the position of the interface between the flows with and without latrunculin.

(B) Image of the same cell after latrunculin B (1 μg/ml) was allowed to flow over the right region as shown in (A), and medium was allowed to flow over the left region, for 15 min. The positions of the mitochondria and the nucleus have shifted toward the left. Arrows show the position of the nucleus before (red) and after (blue) latrunculin treatment.

We used PARTCELL to localize latrunculin B—a membrane-permeable molecule that disrupts actin filaments by binding to actin monomers [26]—to a subcellular domain (Figure 3; a similar experiment using different reagents is also reported in [8]). Local reorganization of cytoskeletal architecture is important for cell movement, as well as for mechanotransduction [27]. The physiological process of actin reorganization involves various intracellular proteins that sequester actin monomers [28],

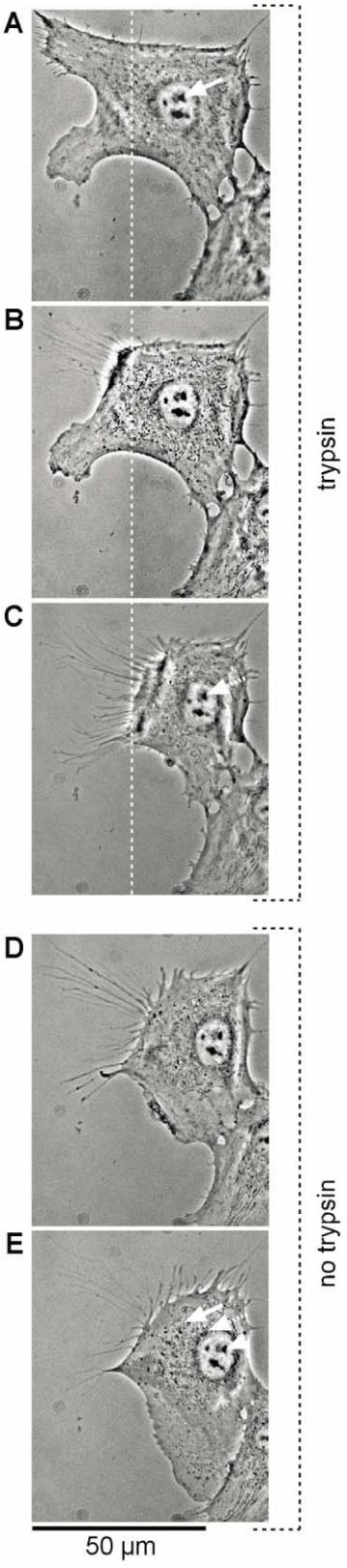

Figure 4. Detachment and Respreading of a BCE Cell after Digestion of a Portion of its Underlying Extracellular Matrix Protein with Trypsin

(A) Cell before treatment with trypsin/EDTA. The left side of this cell was treated with trypsin. The white dotted line indicates the approximate position of the interface between laminar flow paths with and without trypsin; this region was determined by doping the trypsin solution with fluorescent dextran, a noninteracting polymer.

(B) After 1 min of trypsin treatment.

(C) After 3.5 min of trypsin treatment. Trypsin treatment was stopped at this point. The position of the nucleus had shifted significantly to the right as the left part of the cell detached.

(D and E) 40 min (D) and 2 hr (E) after stopping trypsin treatment and replenishing with medium. The arrows represent the position of the nucleus before trypsin treatment (solid line arrow), after trypsin treatment (dashed line arrow), and after 2 hr of respreading (arrowhead only).

break actin filaments [29, 30], and nucleate actin filament growth [31, 32]. PARTCELL allows use of membrane-permeable small molecules to mimic the subcellular activity of such proteins. Sequestration of actin monomer in the right-hand region of the cell by delivering latrunculin B using PARTCELL led to localized actin disruption. This disruption caused the mitochondria, which were made fluorescently visible by transfection of the cell with a fusion construct containing the gene for enhanced yellow fluorescent protein (EYFP) and the mitochondrial targeting sequence from human cytochrome C oxidase, and the nucleus to shift to the left, even though the observed peripheral shape of the cell was relatively unchanged (Figure 3, arrows). The displacement of mitochondria, which are mainly associated with microtubules [33], by local disruption of actin microfilaments is consistent with the existence of mechanical connections between these two types of cytoskeletal filaments; it is also compatible with the conjecture that this composite network exists in a state of isometric tension [27].

PARTCELL can also modify the substrate to which cells are attached. We have previously reported trypsin-mediated detachment of part of a cell using multiple laminar flows [16]. Figure 4 shows an experiment where the process of detachment of a part of a BCE cell with trypsin/EDTA was observed in more detail, and the cell reattachment process was also investigated. Cell surface proteins and extracellular matrix (ECM) proteins adsorbed to the channel floor were proteolytically cleaved in the treated region, and the cell detached from the substrate specifically in the trypsin-treated part; the untreated region was not affected. The nucleus and mitochondria recoiled to the right as the cell reorganized (Figures 4B and 4C, arrows). When the digestion was stopped through replacement of the trypsin-containing stream with serum-containing medium, the cell respread (Figures 4D and 4E). Subcellular ECM digestion is physiologically important in cell migration processes, and increased protease expression has been reported to correlate with increased cellular migration in normal as well as abnormal events such as cancer invasion [34]. PARTCELL provides a new method, with subcellular resolution, for studying ECM proteolysis and cell migration.

PARTCELL can treat the surface of cells with different reagents. We performed two demonstrations using a colloidal particle and a protein. Figure 5A shows area-selective delivery of fluorescently labeled, acetylated, low-density lipoprotein (DiI-Ac-LDL), a colloidal particle,

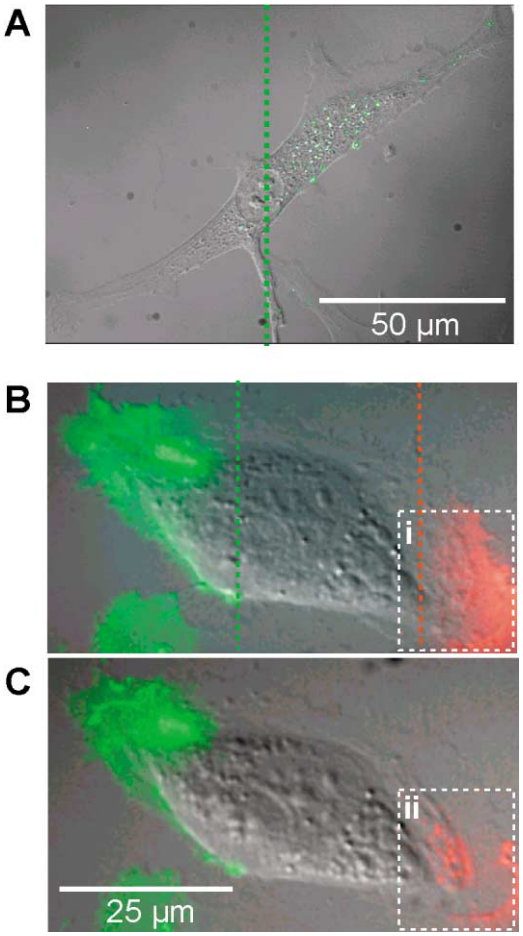

Figure 5. Treating Portions of the Surface of a Cell with Different Reagents

(A) Area-selective delivery of fluorescently labeled, acetylated, low-density lipoprotein (DiI Ac-LDL, Molecular Probes) to a portion of the cell surface. Overlay of fluorescence (dehazed and color enhanced to reproduce the colors perceived visually by microscopy) and differential interference contrast (DIC) micrographs of this cell after DiI-Ac-LDL treatment. The green dotted line indicates the position of the interface between the flows, with and without DiI Ac-LDL. (B–D) Intracellular transport of cell-surface glycoproteins labeled with wheat germ agglutinin (WGA) conjugated to different fluorescent markers. (B) An overlay of fluorescence (color enhanced to reproduce original colors) and DIC micrographs of a BCE cell that had specific microdomains labeled sequentially with green and red fluorescence-labeled WGA. The part of the cell on the left side of the green dotted line was treated with Alexa 488-WGA (0.5 mg/ml, 5 min), and the part of the cell on the right side of the red dotted line was treated with TRITC-WGA (0.5 mg/ml, 5 min). (C) An overlay of fluorescence and DIC micrographs of this cell 1 hr after the WGA treatment. Comparison of regions indicated by white dotted lines in (B) and (C): (1) immediately after being treated with TRITC-WGA, the right tip of the cell was evenly labeled with red fluorescence; (2) 1 hr later, the red fluorescence was concentrated to a number of select locations within the cell. This punctate pattern is indicative of endocytosis of the TRITC-WGA-labeled glycoproteins (also see Supplemental Data).

to the cell surface. We allowed two streams of media—one containing and one lacking DiI-Ac-LDL (Molecular Probes)—to flow over defined regions of a BCE cell; this procedure delivered DiI-Ac-LDL to receptors on the exposed region of the cell surface (Figure 5A). Figures 5B and 5C show the spatially selective endocytosis of cell-surface glycoproteins labeled with wheat germ agglutinin (WGA), a protein. Two different fluorescently labeled WGA solutions (tetramethylrhodamine-labeled WGA [TRITC-WGA] and Alexa 488-labeled WGA [Alexa 488-WGA]) were allowed to flow over opposite ends of a BCE cell. This procedure resulted in the generation of three different populations of cell surface glycoproteins: green fluorescent-labeled, red fluorescent-labeled, and nonlabeled (Figure 5B). Observation of this cell over a 1 hr period showed significant cellular transport of the red fluorescence-labeled glycoproteins (Figures 5E and 5F; also see Supplementary Data), demonstrated by the evolution of a punctate pattern of fluorescence (microvesicles) from a diffuse one. A recent report has also used PARTCELL to deliver epidermal growth factor (EGF) to parts of a cell surface to study ligand-independent lateral propagation of EGF signals [15]. Ligand-independent lateral propagation of signals was observed in cells expressing high densities of EGF receptors, but it was suppressed in cells expressing lower densities of the receptor through endocytosis-mediated removal of activated EGF receptors from the cell surface [15]. Because PARTCELL can deliver molecules to the cell surface in soluble form, dynamic processes such as endocytosis of the molecules delivered to the surface can proceed and be observed in a physiologically relevant manner. This method of localized delivery has an advantage over the technique most commonly used for such studies, which relies on reagents immobilized onto nondiffusive microspheres [6]. The spheres are large (micrometers) compared to the size of the cellular machinery (nanometers), and it is conceivable that they can significantly alter subcellular processes such as endocytosis [6].

Significance

PARTCELL provides a practical method of delivering various reagents—molecules, colloids, or particles—to defined parts of a cell. Its ability to localize rapidly diffusing, membrane-permeable molecules to a part of the cell interior is counterintuitive, given the small size of cells. It is possible because PARTCELL allows rapid influx of molecules to one region of a cell and efflux from another portion of a cell to establish and maintain a chemical concentration gradient inside of the cell. PARTCELL also provides advantages for treating parts of the surface of cells with reagents. Because the technique can perform localized delivery using reagents in their soluble form—that is, without immobilization onto microspheres—dynamic subcellular processes involving the delivered reagents proceed under more physiological conditions than they do using other techniques for localized delivery. PARTCELL requires no equipment or materials that are not commonly found in biological laboratories, except for a mold to form the capillary channels; this mold is easily fabricated [35]. We believe that the technique will be useful in studies of cell dynamics, chemotaxis, cell polarity, spatially regulated signaling, drug screen-

ing, and other phenomena involving intracellular compartments and subcellular heterogeneity.

Experimental Procedures

Reagents

Mitotracker Green FM, Hoechst 33342, Cascade blue-dextran, Styo 9, Alexa Fluor 594 Phalloidin, DiI-Ac-LDL, wheat germ agglutinin tetramethylrhodamine conjugate, and wheat germ agglutinin Alexa Fluor 488 conjugate were purchased from Molecular Probes. Latrunculin B was purchased from Calbiochem. Trypsin/EDTA (0.05% trypsin/0.53 mM EDTA) was obtained from GIBCO.

Capillary Fabrication

A negative relief of the PDMS channel system was formed by curing the prepolymer (Sylgard 184, Dow Corning) on a silanized silicon master having a positive relief (50 μm thickness) of the channels formed in photoresist (SU-8-50, MicroChem) on its surface [35]. The microchannel system required for PARTCELL was prepared by placing the PDMS slab with channel features (300 $\times$ 50 μm) on a glass coverslip (No. 1, Corning; 22 $\times$ 22 mm); the PDMS and the coverslip came into conformal contact to form a seal.

Cell Culture in Capillaries

Before seeding cells, the capillary channels were autoclaved, the inlet reservoirs filled with a protein solution (50 μg/ml fibronectin in phosphate-buffered saline [PBS]), and the system initially aspirated at the outlet to coat the channel walls with fibronectin and make them hydrophilic. Subsequent pumping of fluid was performed gravitationally: the inlet reservoirs were filled with $\sim$100 μl of fluid, and the fluid allowed to flow to the outlet reservoir where the liquid level was kept low by constant removal using a paper tip. One filling was sufficient to maintain flows for an hour. The positions of the different streams were visualized by fluorescence microscopy; when using reagents that were not by themselves fluorescent, we added Cascade blue-dextran (0.5 mg/ml) to the solutions to visualize the streams.

BCE cells were cultured and harvested as previously reported [36]. In brief, cells were cultured under 10% CO_2 on Petri dishes (Falcon) coated with gelatin in Dulbecco's modified Eagle's medium (DMEM, GIBCO) containing 10% calf serum, 2 mM glutamine, 100 μg/ml streptomycin, 100 μg/ml penicillin, and 1 ng/ml basic fibroblast growth factor (bFGF). Cells were dissociated from culture plates with trypsin/ethylenediaminetetraacetic acid (EDTA) and washed in DMEM containing 1% w/v BSA (BSA/DMEM). These cells were suspended in this culture medium and introduced into capillaries from the reservoirs and incubated in 10% CO_2 at 37°C for 6–24 hr prior to performing PARTCELL experiments, which used CO_2-independent medium from GIBCO BRL, with 10% calf serum (CS) and glutamine-penicillin-streptomycin solution (GPS).

Cell Transfection

Fusion constructs containing the gene for enhanced yellow fluorescent protein (EYFP) and the mitochondrial targeting sequence from human cytochrome C oxidase (pEYFP-Mito; Clonetech) were transfected into BCE cells in Figure 3 using the Effectene (Qiagen) technique of liposomal delivery.

Imaging

Cells were observed with an inverted microscope (Nikon Diaphot 300), and the images were captured through a black and white CCD camera (Hamamatsu Orca-100) using image analysis software (IP Lab, www.scanalytics.com). The fluorescent images of mitochondria in Figures 1 and 3 and the fluorescent image of DiI Ac-LDL in Figure 5 were dehazed using Microtome (www.vaytek.com) software, which mathematically calculates and removes out-of-focus background fluorescence or haze.

Supplemental Data

Data from an additional experiment on treating the cell surface with fluorescently labeled WGA and observing microcompartmental endocytosis of the labeled WGA is available. Please write to chembiol@cell.com for a PDF.

Acknowledgments

This work was supported by grants from NIH (GM30367 and CA 45548), NSF ECS-9729405, a fellowship from the Leukemia and Lymphoma Society (S.T.), and a predoctoral fellowship from Glaxo-Wellcome Inc (E.O.). We thank Professor Howard Stone, Abe Stroock (both from Harvard University), and Dr. Sui Huang (Harvard Medical School) for helpful discussion and Dr. Wolfgang Goldman (Harvard Medical School) for assistance with microinjection studies.

Received: June 24, 2002
Revised: December 23, 2002
Accepted: January 6, 2003

References

1. Hartwell, L.H., Hopfield, J.J., Liebler, S., and Murray, A.W. (1999). From molecular to modular cell biology. Nature Suppl. *402*, c47–c52.
2. Pines, J. (1999). Four-dimensional control of the cell cycle. Nat. Cell Biol. *1*, E73–E79.
3. Ashkin, A., and Dziedzic, J.M. (1989). Internal cell manipulation using infrared laser traps. Proc. Natl. Acad. Sci. USA *86*, 7914–7918.
4. Adams, S.R., and Tsien, R.Y. (1993). Controlling cell chemistry with caged compounds. Annu. Rev. Physiol. *55*, 755–784.
5. Blatter, L.A., and Wier, W.G. (1990). Intracellular diffusion, binding, and compartmentalization of the fluorescent calcium indicators indo-1 and fura-2. Biophys. J. *58*, 1491–1499.
6. Brock, R., and Jovin, T.M. (2001). Heterogeneity of signal transduction at the subcellular level: microsphere-based focal EGF receptor activation and stimulation of Shc translocation. J. Cell Sci. *114*, 2437–2447.
7. Bradke, F., and Dotti, C.G. (1999). The role of local actin instability in axon formation. Science *283*, 1931–1934.
8. Takayama, S., Ostuni, E., LeDuc, P., Naruse, K., Ingber, D.E., and Whitesides, G.M. (2001). Laminar flows: subcellular positioning of small molecules. Nature *411*, 1016.
9. Tokeshi, M., Minagawa, T., and Kitamori, T. (2000). Integration of a microextraction system on a glass chip: ion-pair solvent extraction of Fe(II) with 4,7-diphenyl-1,10- phenanthrolinedisulfonic acid and tri-n-octylmethylammonium chloride. Anal. Chem. *72*, 1711–1714.
10. Brody, J.P., Yager, P., Goldstein, R.E., and Austin, R.H. (1996). Biotechnology at low Reynolds numbers. Biophys. J. *71*, 3430–3441.
11. Brody, J.P., and Yager, P. (1997). Diffusion-based extraction in a microfabricated device. Sens. Actuator A *58*, 13–18.
12. Wiegl, B.H., and Yager, P. (1999). Microfluidic diffusion-based separation and detection. Science *283*, 346–347.
13. Takayama, S., Ostuni, E., Qian, X., McDonald, J.C., Jiang, X., LeDuc, P., Wu, M.-H., Ingber, D.E., and Whitesides, G.M. (2001). Topographical micropatterning of poly(dimethlysiloxane) using laminar flows of liquids in capillaries. Adv. Mat. *13*, 570–574.
14. Kenis, P.J.A., Ismagilov, R.F., and Whitesides, G.M. (1999). Microfabrication inside capillaries using multiphase laminar flow patterning. Science *285*, 83–85.
15. Sawano, A., Takayama, S., Matsuda, M., and Miyawaki, A. (2002). Lateral propagation of EGF signaling after local stimulation is dependent on receptor density. Dev. Cell *3*, 245–257.
16. Takayama, S., McDonald, J.C., Ostuni, E., Liang, M.N., Kenis, J.A., Ismagilov, R.F., and Whitesides, G.M. (1999). Patterning cells and their environments using multiple laminar fluid flows in capillary networks. Proc. Natl. Acad. Sci. USA *96*, 5545–5548.
17. Kamholz, A.E., Weigl, B.H., Finlayson, B.A., and Yager, P. (1999). Quantitative analysis of molecular interaction in a microfluidic channel: the T-sensor. Anal. Chem. *71*, 5340–5347.
18. Ismagilov, R.F., Stroock, A.D., Kenis, P.J.A., Whitesides, G., and Stone, H.A. (2000). Experimental and theoretical scaling laws for transverse diffusive broadening in two-phase laminar flows in microchannels. Appl. Phys. Lett. *76*, 2376–2378.
19. Beard, D.A. (2001). Taylor dispersion of a solute in a microfluidic channel. J. Appl. Phys. *89*, 4667–4669.

20. Rajfur, Z., Roy, P., Otey, C., Romer, L., and Jacobson, K. (2002). Dissecting the link between stress fibres and focal adhesions by CALI with EGFP fusion proteins. Nat. Cell Biol. *4*, 286–293.
21. Collins, T.J., Berridge, M.J., Lipp, P., and Bootman, M.D. (2002). Mitochondria are morphologically and functionally heterogeneous within cells. EMBO J. *21*, 1616–1627.
22. Atkins, P.W. (1988). Physical Chemistry, Sixth Edition (New York: Freeman).
23. Mastro, A.M., Babich, M.A., Taylor, W.D., and Keith, A.D. (1984). Diffusion of small molecules in the cytoplasm of mammalian cells. Proc. Natl. Acad. Sci. USA *81*, 3414–3418.
24. Crank, J. (1975). The Mathematics of Diffusion, Second Edition (Oxford: Oxford University Press).
25. Blum, J.J., Lawler, G., Reed, M., and Shin, I. (1989). Effect of cytoskeletal geometry on intracellular diffusion. Biophys. J. *56*, 995–1005.
26. Ayscough, K. (1998). Use of Latrunculin-A, an actin monomer-binding drug. Methods Enzymol. *298*, 18–25.
27. Wang, N., Naruse, K., Stamenovic, D., Fredberg, J., Mijailovic, S.M., Maksym, G., Tolic-Norrelykke, I.M., Polte, T., Mannix, R., and Ingber, D.E. (2001). Mechanical behavior in living cells consistent with the tensegrity model. Proc. Natl. Acad. Sci. USA *98*, 7765–7770.
28. Huff, T., Muller, C.S.G., Otto, A.M., Netzker, R., and Hannappel, E. (2001). Beta-thymosins, small acidic peptides with multiple functions. Int. J. Biochem. Cell Biol. *33*, 205–220.
29. Bamburg, J.R., McGough, A., and Ono, S. (1999). Putting a new twist on actin: ADF/cofilins modulate actin dynamics. Trends Cell Biol. *9*, 364–370.
30. Moriyama, K., and Yahara, L. (2002). The actin-severing activity of cofilin is exerted by the interplay of three distinct sites on cofilin and essential for cell viability. Biochem. J. *365*, 147–155.
31. Pantaloni, D., Le Clainche, C., and Carlier, M.F. (2001). Cell biology—mechanism of actin-based motility. Science *292*, 1502–1506.
32. Pruyne, D., Evangelista, M., Yang, C.S., Bi, E.F., Zigmond, S., Bretscher, A., and Boone, C. (2002). Role of formins in actin assembly: nucleation and barbed-end association. Science *297*, 612–615.
33. Ball, E.H., and Singer, S.J. (1982). Mitochondria are associated with microtubules and not with intermediate filaments in cultured fibroblasts. Proc. Natl. Acad. Sci. USA *79*, 123–126.
34. Xu, J.S., Rodriguez, D., Petitclerc, E., Kim, J.J., Hangai, M., Yuen, S.M., Davis, G.E., and Brooks, P.C. (2001). Proteolytic exposure of a cryptic site within collagen type IV is required for angiogenesis and tumor growth in vivo. J. Cell Biol. *154*, 1069–1079.
35. Duffy, D.C., McDonald, J.C., Schueller, O.J.A., and Whitesides, G.M. (1998). Rapid prototyping of microfluidic systems in poly (dimethylsiloxane). Anal. Chem. *70*, 4974–4984.
36. Ingber, D.E., and Folkman, J. (1989). Mechanochemical switching between growth and differentiation during fibroblast growth factor-stimulated angiogenesis in vitro—role of extracellular-matrix. J. Cell Biol. *109*, 317–330.